

1-13-2003

High-field magnetic resonant properties of β' -(ET)₂SF₅CF₂SO₃

Gary L. Gard
Portland State University

Rolf Walter Winter
Portland State University

J. A. Schlueter

Brian H. Ward

E. Jobiliong

See next page for additional authors

Let us know how access to this document benefits you.

Follow this and additional works at: http://pdxscholar.library.pdx.edu/chem_fac

 Part of the [Physics Commons](#)

Citation Details

I.B. Ruetel, S.A. Svyagin, J.S. Brooks, J. Krzystek, P. Kuhns, A.P. Reyes, B.H. Ward, J.A. Schlueter, and R.W. Winter, High-Field Magnetic Resonant Properties of β' -(ET)₂SF₅CF₂SO₃, *Phys. Rev. B*, 67, 214417 (2003).

This Article is brought to you for free and open access. It has been accepted for inclusion in Chemistry Faculty Publications and Presentations by an authorized administrator of PDXScholar. For more information, please contact pdxscholar@pdx.edu.

Authors

Gary L. Gard, Rolf Walter Winter, J. A. Schlueter, Brian H. Ward, E. Jobiliong, A. P. Reyes, P. Kuhns, J. Krzystek, J. S. Brooks, S. A. Zvyagin, and B. Rutel

High-field magnetic resonant properties of β' -(ET)₂SF₅CF₂SO₃I. B. Rutel,¹ S. A. Zvyagin,¹ J. S. Brooks,¹ J. Krzystek,¹ P. Kuhns,¹ A. P. Reyes,¹ E. Jobilong,¹ B. H. Ward,²
J. A. Schlueter,³ R. W. Winter,⁴ and G. L. Gard⁴¹National High Magnetic Field Laboratory and Physics Department, Florida State University, Tallahassee, Florida 32310, USA²Florida State University, Department of Chemistry and Biochemistry, Tallahassee, Florida 32306-4390, USA³Materials Science Divisions, Argonne National Laboratory, Argonne, Illinois 60439-4831, USA⁴Department of Chemistry, Portland State University, Portland, Oregon 97207-0751, USA

(Received 22 October 2002; revised manuscript received 31 March 2003; published 13 June 2003)

The charge transfer salt β' -(ET)₂SF₅CF₂SO₃, which has previously been considered a spin-Peierls material with a $T_{SP} \sim 33$ K, is examined using high-resolution high-field sub-millimeter/millimeter wave electron spin resonance (ESR), and nuclear magnetic resonance (NMR) techniques. A peak in the nuclear spin-lattice relaxation behavior in fields of 8 T, accompanied by a broadening and paramagnetic shift of the resonance line, indicates a phase transition at $T_c \sim 20$ K. A pronounced change in the high-field ESR excitation spectra at ~ 24 T, observed at $T_c \sim 20$ K, may indicate the onset of antiferromagnetic (AFM) correlations of the low-temperature phase in β' -(ET)₂SF₅CF₂SO₃. Peculiarities of the low-temperature magnetic and resonance properties of β' -(ET)₂SF₅CF₂SO₃ are discussed.

DOI: 10.1103/PhysRevB.67.214417

PACS number(s): 74.25.Fy, 72.15.Jf, 75.30.Kz

I. INTRODUCTION

The (ET)₂ X charge transfer salts represent a large number of materials that possess properties ranging from insulator to superconductor [ET is bis(ethylenedithio)tetrathiofulvalene]. The same can be said for the subclass of compounds (ET)₂SF₅RSO₃, where $R = \text{CH}_2, \text{CF}_2, \text{CHF}, \text{CH}_2\text{CF}_2$.¹ Modifications of the anion result in fundamental changes in the structural and physical properties, and investigations on these materials have been pursued to determine the relation of the anion to the material behavior. Some interest is focused on the anion relation to the conduction path formed by π - π orbital overlap of sulfur in the ET donor molecules.²⁻⁸ The role of the anion in electrical properties is still unclear. However, it is certain that the anion plays a role in partially determining the structure of the compound and accepting an electron from the ET molecule, forming a potential conduction hole. The hole then promotes the spin character of the system, providing magnetic interaction through band magnetism. It is interesting to investigate such systems that show a transition of a low dimensional magnetism into a three dimensional (3D) AFM state, as well as those which exhibit a transition into a spin-Peierls state.

β' -(ET)₂SF₅CF₂SO₃ is characterized by pairs of (ET)^{+1/2} molecules which contribute a single electron to the SF₅CF₂SO₃⁻¹ anion acceptor, forming a charge transfer salt, which stacks with face-to-face ET contacts (Fig. 1). The ET dimers form linear spin chains along the b axis.⁹

A measurement of the superconducting quantum-interface device (SQUID) susceptibility for β' -(ET)₂SF₅CF₂SO₃ (Fig. 2) shows a broad maximum at $T \approx 115$ K, indicating the low dimensional character of the interactions.

The susceptibility was fit using the Bonner-Fisher model for $S = \frac{1}{2}$ Heisenberg antiferromagnet (HAF).¹⁰ The best fit for $T > 40$ K was obtained using a coupling constant $J/k_B = 352$ K. Thus, the Bonner-Fisher fit together with a crystal

structure analysis suggest a $S = \frac{1}{2}$, linear magnetic chain.¹¹

A kink in the susceptibility is observed at $T \sim 45$ K (which was suggested to be a spin-Peierls transition temperature¹), followed by a pronounced drop at $T \sim 20$ K. As temperature drops below 20 K there is an intrinsic feature which makes it difficult to reveal the nature of the ground state in the low temperature regime. Previous V -band electron spin resonance (ESR) experiments revealed a collapse of the gapless $g \sim 2$ mode below 33 K. The change in the excitation spectrum was interpreted to as possible evidence of the spin-Peierls transition.⁹ A change in the FIR properties was observed below $T \sim 45$ K, which indicate weak lattice distortions in β' -(ET)₂SF₅CF₂SO₃.¹² In order to study the nature of the low-temperature transition in β' -(ET)₂SF₅CF₂SO₃, we decided to perform ESR experiments in an extended frequency-field range, using high-field high-resolution submillimeter/millimeter wave ESR spectrometer recently developed at the National High Magnetic Field Laboratory (NHMFL), in Tallahassee, Florida.¹³ In addition, low-temperature properties of β' -(ET)₂SF₅CF₂SO₃ are probed using a pulsed NMR spectroscopy technique.

II. EXPERIMENTAL TECHNIQUES

The ESR method is a powerful tool in studying the nature of the ground states in solids (see, for instance, Refs. 14, 15, and 16). We investigate the β' -(ET)₂SF₅CF₂SO₃ system employing ESR and NMR techniques at high frequencies and magnetic fields. High-resolution ESR was carried out in the 25 T W.M. Keck resistive magnet [with magnetic field homogeneity, 12 ppm/cm density spherical volume (DSV)] at the NHMFL, using backward wave oscillator (BWO) sources. Investigations were performed by holding temperature and frequency constant and sweeping the magnetic field. Details of the high-field millimeter and submillimeter wave facility can be found in Zvyagin and Krzystek.¹³

In our experiments we used single-crystalline samples with a typical size of $0.5 \times 0.1 \times 0.1$ mm³.¹ To measure such

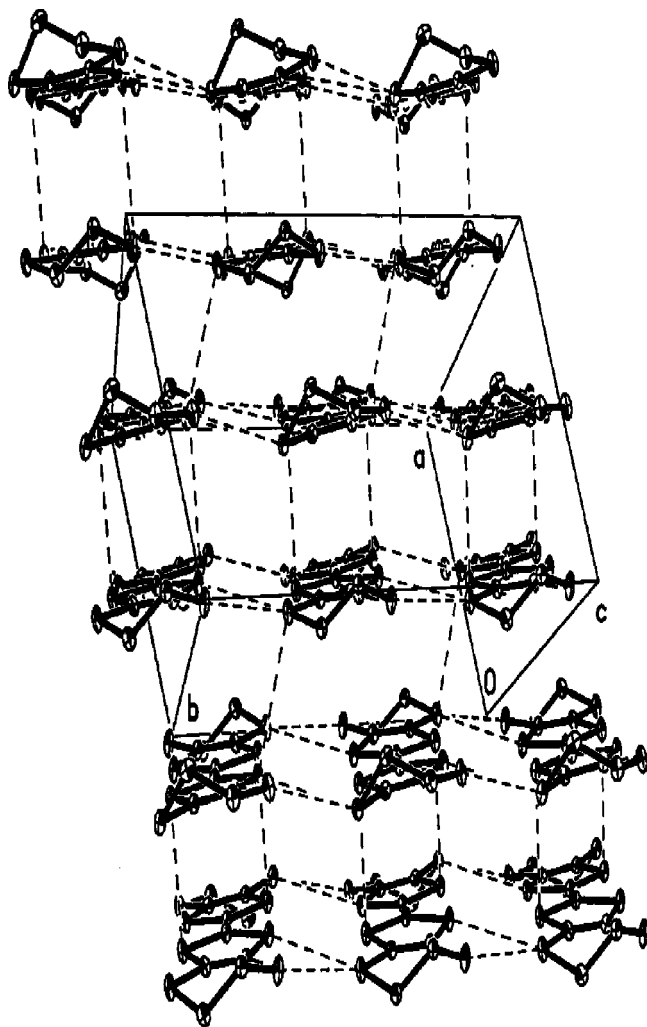


FIG. 1. β' -(*ET*)₂SF₅CF₂SO₃ cation layer. The view is down the long axis of the molecule. Dashed lines between donor stacks indicate S...S van der Waals contacts less than 3.6 Å. The *ET* molecules are dimerized and form linear chains along the *b* axis (Ref. 9). Interstack distances between donors (along *b* axis) are ~ 5.3 Å, while intrastack distances are ~ 7.3 Å. The β' -(*ET*)₂SF₅CF₂SO₃ crystal cell has $P\bar{1}$ symmetry below 120 K, and forms a triclinic unit cell with $a=7.699$ Å, $b=13.151$ Å, $c=17.643$ Å, and $\alpha=81.323^\circ$, $\beta=87.416^\circ$, $\gamma=74.994^\circ$ (Ref. 1).

small samples a special sample holder was built. It consists of two metallic horns, conically reducing the microwave radiation down to the sample size (Fig. 3). A metallic foil was placed around the sample to reduce noise caused by background radiation. The sample was placed in the Faraday configuration, i.e., the propagation vector of the radiation \vec{k}_ω is parallel to the external magnetic field \mathbf{H} . An optical chopper was used to modulate the microwave power. \mathbf{H} was oriented perpendicular to the *c* axis of the sample. The probe was coupled to the source via circular waveguide sections and directed into the sample space, where the microwave excitation passed through the sample, a polymer platform, and then a marker compound of DPPH (2,2-diphenyl-1-picrylhydrazyl). The radiation was then directed out of the probe and into a helium cooled InSb detector.

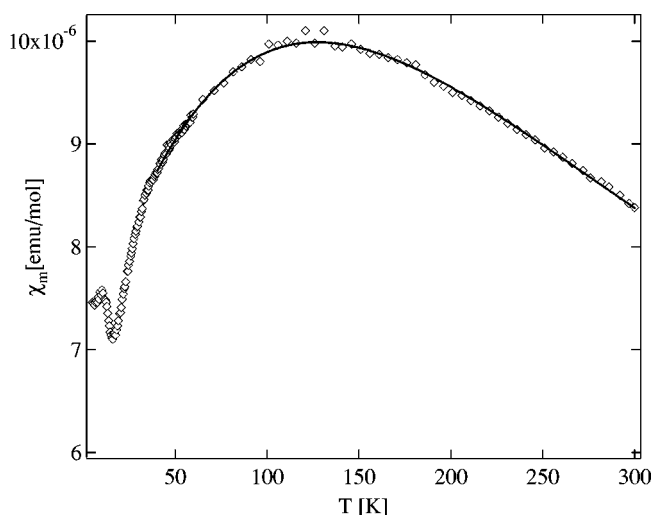


FIG. 2. Magnetic susceptibility versus temperature for β' -(*ET*)₂SF₅CF₂SO₃. Solid curve is a Bonner-Fisher theory fit for $S=\frac{1}{2}$ HAF.

NMR investigations were performed in a 15 T superconducting magnet. A home-built MagRes2000 spectrometer¹⁷ and a capacitively tuned and matched probe were employed. The investigation focused on two nuclei, the ¹⁹F nucleus on the anion and ¹H in the ethylene groups on the donor molecule (*ET*). Remarkably, the NMR results revealed similar behavior for these two sites which are also independent of field (or frequency), suggesting a common mechanism for the spin dynamics at the anion layer and at the *ET* molecule. For brevity, we present a representative graph showing the results of the 340 MHz (8 T) investigation of the ¹H nuclei.

III. RESULTS AND DISCUSSION

We first present the NMR data performed in the temperature range ~ 3 –300 K and show evidence indicating that the transition seen at $T\sim 20$ K is not spin-Peierls in nature. The characteristic behavior of the nuclear spin-lattice relaxation rate (T_1^{-1}) in a prototypical spin-Peierls material CuGeO₃ is

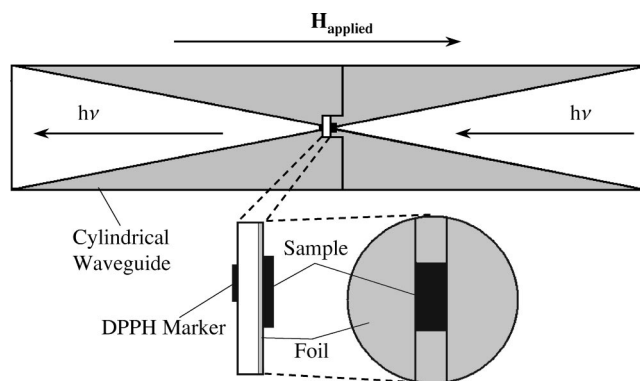


FIG. 3. Direct transmission ESR sample holder. The microwave radiation is conically reduced to the sample size. The sample is placed on a polymer holder with metallic masking to block any radiation not passing through the sample. The marker, DPPH, is placed on the side of the holder opposite from the sample.

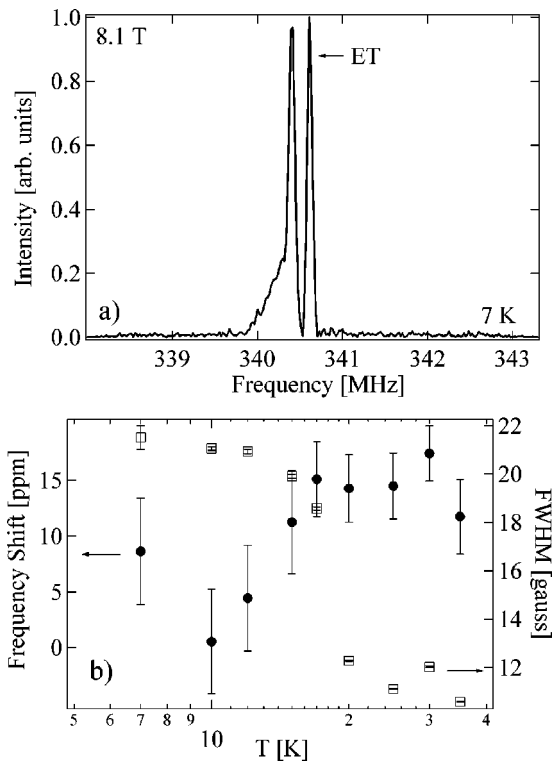


FIG. 4. (a) NMR spectra for ^1H at 340.61 MHz. The line marked “*ET*” is the signal from the sample, and the second line at lower field is an off resonance spurious signal from the probe. (b) The hyperfine magnetic shift (left axis) for the β' -(*ET*)₂SF₅CF₂SO₃ material, determined from the spectral shift away from the carrier frequency in the NMR investigation, and the full width at half maximum (FWHM) analysis (right axis) of the spectral line for the title compound from the NMR spectra.

described in Ref. 18. Above the transition temperature T_{sp} , where the system would be in a uniform phase, the fluctuations from weakly interacting spins contributes to a large but weakly temperature-dependent relaxation rate. In CuGeO₃,¹⁸ this behavior persists until the temperature drops below T_{sp} , where T_1^{-1} decreases sharply (by several orders of magnitude). There is also a change in the magnetic hyperfine shift which follows the T_1^{-1} curve, decreasing below the transition temperature.

A typical NMR ^1H spectrum in β' -(*ET*)₂SF₅CF₂SO₃ is shown in Fig. 4(a), taken at 8.1 T. The data for ^{19}F NMR is not shown. The ^1H data show a narrow *ET* signal and a spurious signal at a lower frequency. This second signal originates from the probe which was difficult to eliminate completely. This signal has a much longer T_1 than the *ET* signal and remains well resolved and separated throughout the investigation.

In Fig. 5 we show the temperature dependence of ^1H T_1^{-1} . At high temperatures, the relaxation rate is slightly temperature-dependent. As the temperature is lowered, instead of the expected drop at T_{sp} , we observed a sharp peak reaching a maximum at around 20 K followed by a sudden drop at lower temperatures. Concomitantly, the FWHM, shown in Fig. 4(b), also increases around 20 K, while the resonance frequency [Fig. 4(b)] drops. These data are sug-

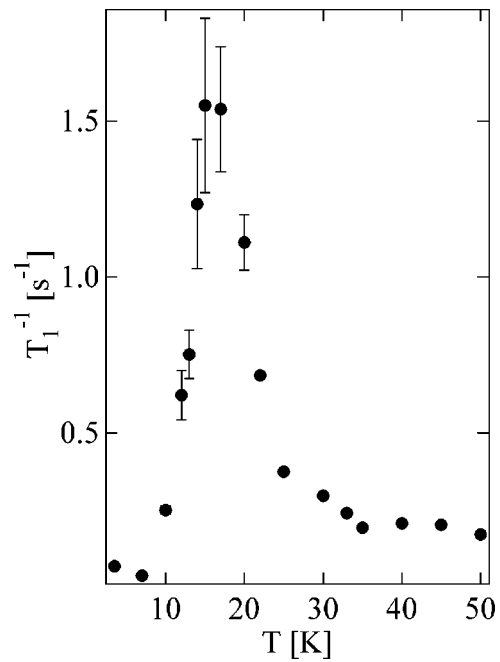


FIG. 5. The NMR data for the spin-lattice relaxation (T_1^{-1}) plotted versus temperature for ^1H at 360 MHz. This investigation clearly shows non-spin-Peierls behavior. See text for details.

gestive of some form of magnetic order. Indeed, this sample shows remarkably similar behavior to the LiMn₂O₄ system, a material with an AFM ground state.

The data for the ^{19}F NMR (not shown) also reveals the same peak in T_1^{-1} at the same temperature. The similarity in these behavior at two different sites, both the ^1H and ^{19}F (on the *ET* molecule and anion respectively), suggests that the relaxation at both sites is dominated by a single spin dynamics.¹¹

A representative transition to an AFM phase is given by Sugiyama *et al.* in the LiMn₂O₄ system.¹⁹ In the case of AFM ordering a peak is found in the T_1^{-1} scattering with the Néel temperature (T_N) indicated by the maximum of the peak. Both the full width at half maximum (FWHM) and the magnetic hyperfine shift show increases at T_N .

Generally, a 3D antiferromagnetic ordering produces large hyperfine fields at the nuclear site, thus shifting the resonance and rendering the NMR line unobservable in the detected frequency range. In the present case, the signal remains tractable down to the lowest temperature measured. This may occur if the ordering is not long-ranged in nature or if the sample is not uniform, which is unlikely. It is also important to note that the bulk susceptibility does not show any direct signature of AFM ordering. In addition, although the FWHM follows the correct trend, it is two orders of magnitude smaller than the LiMn₂O₄ data. Nevertheless and whatever the case maybe, it is clear from the NMR data the absence of any transition at T_{sp} (~ 40 K) and that the anomaly at ~ 20 K is definitely something other than a spin-Peierls transition.

We now present a discussion of the ESR investigation. In the case of the low-frequency ESR (*V* band and *W* band) we have a single resonance line which remains relatively con-

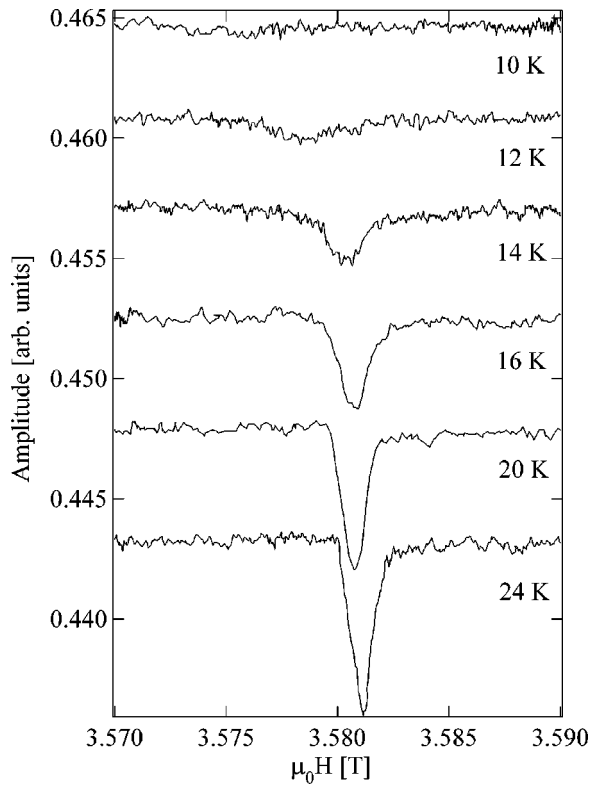


FIG. 6. Data from ESR performed at 98 GHz and 3.5 T. The run was performed on the same sample as the high-frequency investigation, after the BWO experiment. The data show reliable reproducibility for the low-frequency behavior of the $\beta'-(\text{ET})_2\text{SF}_5\text{CF}_2\text{SO}_3$ sample.

stant in width, amplitude, and frequency above 20 K and shows a diminishing amplitude, slight broadening, and small shift to lower field below 20 K. The resonance field data, $H\parallel c$ axis also show a relatively constant value with a slight change to lower field below 20 K.⁹ The experiment was repeated using the sample investigated in both the NMR and high-frequency ESR (see below). Figure 6 reports data taken at 98 GHz, where similar shifts, broadening, and diminishing amplitude are evidence for the reproducibility of the previous investigation.⁹

This behavior is quite different from that observed at the higher frequency and field. We first discuss the ESR results seen as the raw data in Fig. 7, which shows the sample response with changing temperature. At higher temperatures we observe one signal, corresponding to the sample absorption. As the temperature decreases we find the sample absorption line broadens and eventually splits, where the onset of the broadening occurs around 20 K. Following the line to lower temperatures, the broadened line begins to resolve into two and then three distinct lines (denoted by arrows 1, 2, and 3 in Fig. 7).

The high-frequency case (broadening followed by splitting) can be explained by the appearance of three AFM modes at some fixed frequency in the fields: below $H_{\text{spin-flop}}$, above $H_{\text{spin-flop}}$ and in an intermediate critical regime at $H \sim H_{\text{spin-flop}}$,²⁰ which were observed experimentally for instance in MnF_2 .²¹ The high-frequency-field data

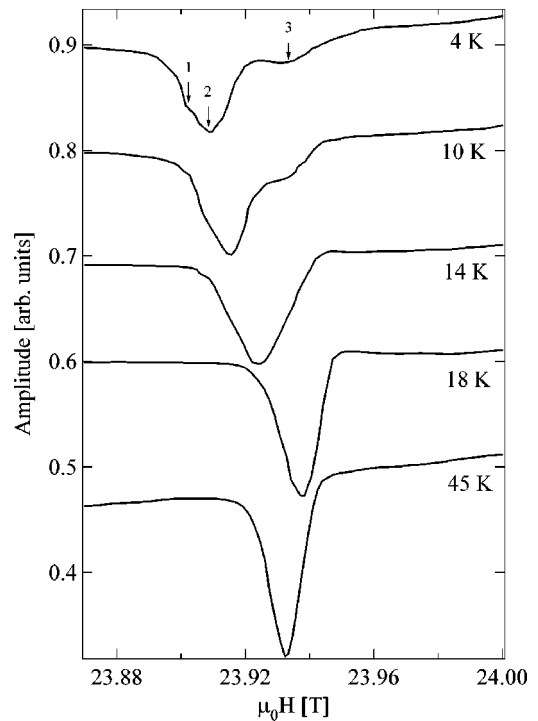


FIG. 7. Raw data from ESR investigation at 673 GHz for varying temperature. The onset of broadening and introduction of new lines with decreasing temperature suggests an AFM ordering observed below the transition. Arrows indicate the multiple resonance lines seen in the investigation. The spectra are offset for clarity.

indicate the appearance of new excitation modes, that may be understood in terms of the model developed for spin excitations in a uniaxial AFM with $H\parallel$ easy axis.²⁰ Of course, tilting of the principal axis (even very small) and a low symmetry ($P1$) of $\beta'-(\text{ET})_2\text{SF}_5\text{CF}_2\text{SO}_3$ can cause some deviations from the model.²⁰

Both sets of data show the onset of a transition at $T \sim 20$ K, where the transition temperature is also verified in the high-frequency data by the onset of splitting and remaining area under the curve seen in Fig. 8 and its inset. However, several pronounced differences appear between the two sets of data. The first difference is the persistence of excitations below about 10 K in the high-frequency data seen in Fig. 8 as opposed to that reported in Ref. 9. Second, the high-frequency data show the splitting of the line at low temperatures (Fig. 8), which may indicate the onset of 3D AFM ordering.

Remarkably, in both cases the behavior is qualitatively similar to that for AFM ordering. The low-frequency case (broadening and shifting) corresponds to similar features reported by Mitsudo *et al.* in LaMnO_3 .²² The broadening is due to 1) the enhancement of the AFM correlations and 2) the change of the frequency-field slope. This leaves us with the conclusion that both the low-frequency and the high-frequency results may suggest an AFM type ordering in $\beta'-(\text{ET})_2\text{SF}_5\text{CF}_2\text{SO}_3$ at low temperature.

We should also make mention of the intrinsic nature of the anomaly in the low- T portion of the susceptibility. Assume that the low- T part of the susceptibility is caused by the

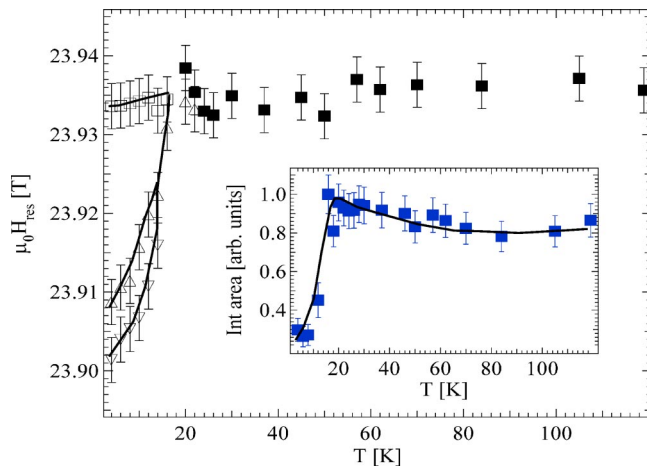


FIG. 8. ESR resonance field versus temperature for β' -(*ET*)₂SF₅CF₂SO₃ oriented with $H \perp c$ axis; the frequency is 673 GHz. Open triangles down and up, and open squares represent the absorption lines denoted by arrows 1, 2, and 3, respectively, below the transition temperature (Fig. 7). Solid squares represent the absorption line in the paramagnetic phase, and solid curves are guides for the eye. Inset: Integrated area of the ESR absorption at the frequency 673 GHz plotted versus temperature. The area is calculated from a multiple Lorentzian fit for absorption lines denoted by squares in Fig. 7. A drop in the integrated intensity is seen below 20 K.

paramagnetic impurities (chain ends, defects, other impurities). This impurity signal (which appears to be nonnegligible in the susceptibility) should manifest itself in the ESR as excitations with $g \sim 2$. We did see the signal from such impurities for $T < 10$ K, where the 98 GHz investigation and Ward *et al.* did not. This suggests that the low- T portion is intrinsic to the system, and may have something to do with the AFM ordering suggested by the ESR.

Let us also discuss the possibility of an incommensurate phase. It is known that if we apply a high field we can enter

into an incommensurate phase, where the magnetic structure is incommensurate with the crystal structure. ESR was studied by Palme *et al.* in the incommensurate phase of the spin-Peierls material CuGeO₃, where hysteresis appears to be a basic property of the system.²³ However, in our investigations we observed no hysteresis. This would again support the non-spin-Peierls nature of the ~ 20 K transition.

IV. CONCLUSION

We investigate β' -(*ET*)₂SF₅CF₂SO₃, employing both pulsed NMR and high-frequency ESR methods. Both the NMR and ESR data provide evidence that the title compound does not exhibit behavior characteristic for a conventional spin-Peierls transition. We submit that both the NMR and the high-frequency ESR investigations provide inconclusive results as to the nature of the ground state in the low- T regime, although there is some evidence of a 3D AFM ordering. It is clear that there is a disparity between the low- and high-frequency/field dependence, but at present no theory appears to describe the behavior fully. Further investigations using x-ray diffraction and neutron scattering could provide insight into a more exact description of the crystallographic and magnetic structure through the $T < 20$ K phase transition.

ACKNOWLEDGMENTS

The FSU acknowledges support from Grant No. NSF-DMR 99-71474 and Grant No. IHRP 500/5031. A portion of this work was performed at the National High Magnetic Field Laboratory, which is supported by NSF Cooperative Agreement No. DMR-0084173 and by the state of Florida. Work at Argonne National Laboratory was supported by the Office of Basic Energy Science, Division of Materials Sciences, U.S. Department of Energy, under Grant No. W-31-109-ENG-38. Research at Portland State University was supported by NSF Grant CHE-09904316.

¹B. H. Ward, J. A. Schlueter, U. Geiser, H. H. Wang, E. Morales, J. P. Parakka, S. Y. Thomas, J. M. Williams, P. G. Nixon, R. W. Winter, G. L. Gard, H.-J. Koo, and M.-H. Whangbo, *Chem. Mater.* **12**, 343 (2000).

²T. Mori, *Bull. Chem. Soc. Jpn.* **71**, 2509 (1998).

³T. J. Emge, H. H. Wang, P. C. W. Leung, P. R. Rust, J. D. Cook, P. L. Jackson, K. D. Carlson, J. M. Williams, M. H. Whangbo, Eugene L. Venturini, James E. Schirber, Larry J. Azevedo, and John R. Ferrarol, *J. Am. Chem. Soc.* **108**, 695 (1986).

⁴T. J. Emge, H. H. Wang, M. K. Bowman, C. M. Pipan, K. D. Carlson, M. A. Beno, L. N. Hall, B. A. Anderson, J. M. Williams, and M. H. Whangbo, *J. Am. Chem. Soc.* **109**, 2016 (1987).

⁵H. Endres, M. Hiller, H. J. Keller, K. Bender, E. Gogu, I. Heinen, and D. Schweitzer, *Z. Naturforsch. B* **40b**, 1664 (1985).

⁶D. Chasseau, S. Hébard, V. Hays, G. Bravic, J. Gaultier, L. Ducasse, M. Kurmoo, and P. Day, *Synth. Met.* **70**, 947 (1995).

⁷P. Day and M. Kurmoo, *J. Mater. Chem.* **7**(8), 1291 (1997).

⁸J. Moldenhauer, C. Horn, K. I. Pokhodnia, I. Heinen, and H. J.

Keller, *Synth. Met.* **60**, 31 (1993).

⁹B. H. Ward, I. B. Rutel, J. S. Brooks, J. A. Schlueter, R. W. Winter, and G. L. Gard, *J. Phys. Chem. B* **105**, 1750 (2001).

¹⁰J. C. Bonner and M. E. Fisher, *Phys. Rev.* **135**, 640 (1964).

¹¹I. B. Rutel, Ph.D. thesis, Florida State University (2002).

¹²J. M. Pigos, B. R. Jones, Z.-T. Zhu, J. L. Musfeldt, C. C. Homes, H.-J. Koo, M.-H. Whangbo, J. A. Schlueter, B. H. Ward, H. H. Wang, U. Geiser, J. Mohtasham, R. W. Winter, and G. L. Gard, *Chem. Mater.* **13**, 1326 (2001).

¹³S. Zvyagin and J. Krzystek, *NHMFL Reports*, Vol. 9, N-3 (2002).

¹⁴M. Dumm, A. Loidl, B. W. Frawel, K. P. Starkey, L. K. Montgomery, and M. Dressel, *Phys. Rev. B* **61**, 511 (2000).

¹⁵M. Dumm, M. Dressel, A. Loidl, B. W. Frawel, K. P. Starkey, and L. K. Montgomery, *Synth. Met.* **103**, 2068 (1999).

¹⁶S. Zvyagin, G. Cao, Y. Xin, S. McCall, T. Caldwell, W. Moulton, L.-C. Brunel, A. Angerhofer, and J. E. Crow, *Phys. Rev. B* **66**, 064424 (2002).

¹⁷A. Reyes, *NHMFL Annual Research Review* **2000**, 255.

- ¹⁸Y. Fagot-Revurat, M. Horvatic, C. Berthier, J. P. Boucher, P. Ség-ransan, G. Dhalenne, and A. Revcolevschi, *Phys. Rev. B* **55**, 2964 (1997).
- ¹⁹S. Sugiyama, T. Hioki, S. Noda, and M. Kontani, *Mater. Sci. Eng., B* **54**, 73 (1998).
- ²⁰E. A. Turov, in *Physical Properties of Magnetically Ordered Crystals* (Academic Press, New York, 1965).
- ²¹M. Hagiwara, K. Katsumata, I. Yamada, and H. Suzuki, *J. Phys.: Condens. Matter* **8**, 7349 (1996).
- ²²S. Mitsudo, K. Hirano, H. Nojiri, M. Motokawa, K. Hirota, A. Nishizawa, N. Kaneko, and Y. Endoh, *J. Magn. Magn. Mater.* **177-181**, 878 (1998).
- ²³W. Palme, G. Ambert, J. P. Boucher, G. Dhalenne, and A. Revcolevschi, *Phys. Rev. Lett.* **76**, 4817 (1996).